# The calculation of stress intensity factors by the surface integral method

Chi-Sub Jin †

*Department of Civil Engineering, Pusan National University, Pusan 609-735, Korea*

Heui-Suk Jang †

*Department of Civil Engineering, Pusan National University of Technology, Pusan 608-080, Korea*

Hyun-Tae Choi ‡

*Research Institute of Industrial Technology, Pusan National University,Pusan 609-735, Korea*

**Abstract.** The determination of the stress intensity factors is investigated by using the surface integral defined around the crack tip of the structure. In this work, the integral method is derived naturally from the standard path integral $J$. But the use of the surface integral is also extended to the case where body forces act. Computer program for obtaining the stress intensity factors $K_I$ and $K_{II}$ is developed, which prepares input variables from the result of the conventional finite element analysis. This paper provides a parabolic smooth curve function. By the use of the function and conventional element meshes in which the aspect ratio (element length at the crack tip/crack length) is about 25 percent, relatively accurate $K_I$ and $K_{II}$ values can be obtained for the outer integral radius ranging from 1/3 to 1 of the crack length and for inner one zero.

## 1. Introduction

In 1928, Richart, *et al.* pronounced for the first time that microcracks are occurred prior to stresses and strains of concrete being sufficiently large to make tension-fracture. Also, Neville (1959) applied Griffith's theory to concrete in the first place, where he insisted on that this theory can be used only approximately in concrete, because concrete's strength might be dependent on not critical stress criterion but critical strain criterion.

In the first experimental paper applying fracture mechanics concept to concrete, Kaplan (1961) concluded that LEFM was adequate failure criterion for concrete by way of bending test of concrete beams that had various crack length. On the other hand, Kesler, *et al.* (1972) tested central cracked plates which were made of mortar and concrete. From the test, they reported that LEFM is not a proper fracture criterion for concrete because of variance of fracture toughness

---

† Professor
‡ Research Associate

according to crack length. But Saouma, et al. (1982) reanalyzed the test results using quarter point singular triangle elements at the crack tip zone, in which they concluded that Kesler, et al's opinion was not valid and LEFM can be applied to concrete in an engineering point of view.

In fact, seeing that property of concrete material, only macroscopic analysis is still useful. But assumption of perfect elasticity for concrete and consideration of linear parts for load-displacement diagram can make nonlinear effects unimportant. Moreover if specimen's size are sufficiently large so that plane strain condition remains, it is thought that fracture property of concrete can be decided by LEFM.

To trace crack propagation by LEFM, first of all, stress intensity factor(SIF) values are to be calculated. Then, from these SIF values, displacements and stresses of crack tip zone can be obtained. Moreover crack propagation can be decided by comparing these values with fracture toughness of the material.

These SIF values can be obtained easily from general formula utilizing stress function in the case of simple geometry. But numerical techniques like finite element method(FEM) must be applied for the case of complicated ones. So, FEM was used as a typical method for obtaining a solution of the fracture problem in the last 20 years.

There are several methods to obtain SIF by FEM. First, SIF can be determined from comparison of theoretical values of displacement field and stress field at the crack tip zone with finite element analysis results (Barsoum 1976, Owen and Fawkes 1983, Jin, Jang, Choi and Eum 1989). But this method requires the use of fine element division and singular elements to represent stress singularity at the crack tip zone. Second, strain energy release rate method (Irwin 1956) and fictitious crack extension method, (Hellen 1975) which requires a FEM analysis for different crack length twice. Third, SIF can be obtained from line integral values which are independent of the used contours, especially Rice's J-integral (1968) has been widely used. But this method has an inconvenience to define the integral contour in advance.

By the way, Babuška and Miller (1984) proposed the surface integral method which can directly calculate SIF $K_I$ and $K_{II}$. But, here, since displacement field of crack tip zone was introduced in asymptotic expansion form, there are some difficulties. Droz (1987) also obtained SIFs by the surface integral method, but quite a few differences with analytical solutions could be seen in his results.

It is the purpose of this paper to introduce surface integral method by modifying conventional J-integral method, to propose special smooth curve function, and finally to make a post-processing program that can easily and more correctly calculate SIF by surface integral method.

## 2. Surface integral method

### 2.1. Surface integral method and stress intensity factor

The surface integral method is based on the energy of the crack tip, strain field and stress field at near the crack tip. So, SIF $K_I$ and $K_{II}$ can be directly obtained by this method in which singular element and fine element division are not necessary. Since this method is very similar to formulation of the J-integral, it is assumed that any body forces are not considered and external forces are not applied to the crack surfaces.

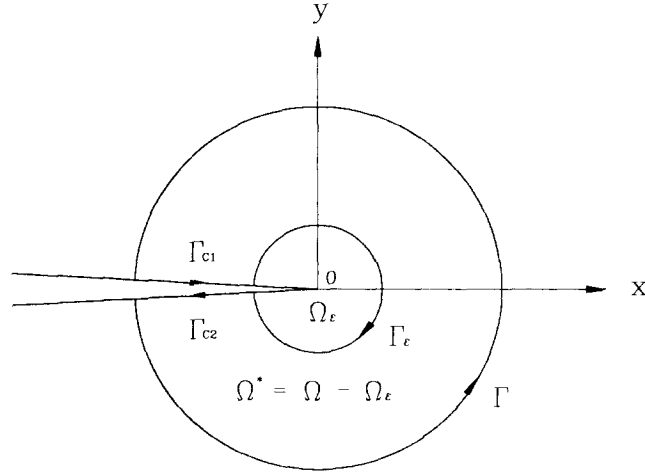In the integral contour and domain of Fig. 1, closed contour $\Gamma^*$ can be defined as follows.

Fig. 1 Contours and domain of surface integral

$$\Gamma^* = \Gamma + \Gamma_{C1} + \Gamma_\varepsilon + \Gamma_{C2} \tag{1}$$

And considering integral direction, $J$-integral for path $\Gamma_\varepsilon$ is as follows.

$$J = -\int_{\Gamma_\varepsilon} (w\,dy - t_i u_{i,1}\ ds) \tag{2}$$

Where $W$ is strain energy density, $t_i$ is traction vector normal to the plane $n$, $U_i$ is displacement vector, and $ds$ is the element of arc along the path $\Gamma$.

Here, any sufficiently smooth function $\phi$ is considered, which has unit value on the contour $\Gamma_\varepsilon$ and in the area $\Omega_\varepsilon$ and has 0 value on the $\Gamma$ contour and outside area of $\Omega$. And from Fig. 1, it can be seen that $dy=0$ in the path $\Gamma_c = \Gamma_{C1} + \Gamma_{C2}$. And considering $\tilde{t}=0$ in the crack surfaces $\Gamma_c$, following expression can be made.

$$\int_{\Gamma_{C1+C2}} (w\,dy - t_i u_{i,1}\,ds)\,\phi = 0 \tag{3}$$

And about contour $\Gamma$, following expression can be written.

$$\int_\Gamma (w\,dy - t_i u_{i,1}\,ds)\,\phi = 0 \tag{4}$$

Therefore, integral about closed contour $\Gamma^*$ can be represented as follows.

$$J = -\int_{\Gamma^*} (wn_1 - t_i u_{i,1})\,\phi\,ds \tag{5}$$

Where $n_1$ is $x$ directional component of outward unit normal vector and is equal to $dy/ds$. Changing Eq. (5) to the surface integral about area $\Omega^*$ by use of the Green's theorem and considering $W = \frac{1}{2}\sigma_{ij}\varepsilon_{ij}$, following expression can be obtained.

$$J = -\frac{1}{2}\int_{\Omega^*} \{(\sigma_{i2}u_{i,2} - \sigma_{i1}u_{i,1})\phi_{,1} - 2(\sigma_{i2}u_{i,1})\phi_{,2}\}\,d\Omega \tag{6}$$

Since displacement $v$ at near the crack tip obtained from FEM analysis can be regarded as a approximate values for the analytical solution $u$, $v$ can be represented as follows.

$$v \approx u = K_I u^I + K_{II} u^{II} \tag{7}$$

where $u^I$, $u^{II}$ are as follows.

$$u^I = \frac{1}{4\mu} \sqrt{\frac{r}{2\pi}} \begin{bmatrix} (2\kappa-1) \cos\frac{\theta}{2} - \cos\frac{3}{2}\theta \\ (2\kappa+1) \sin\frac{\theta}{2} - \sin\frac{3}{2}\theta \end{bmatrix}$$

$$u^{II} = \frac{1}{4\mu} \sqrt{\frac{r}{2\pi}} \begin{bmatrix} (2\kappa+3) \sin\frac{\theta}{2} + \sin\frac{3}{2}\theta \\ -(2\kappa-3) \cos\frac{\theta}{2} - \cos\frac{3}{2}\theta \end{bmatrix} \tag{8}$$

In the above expression, $\mu$ is the shear modulus, $\kappa$ is $(3-v)/(1+v)$ in plane stress condition and $(3-4v)$ in plane strain condition, where $v$ is Poisson's ratio.

A similar expression can be considered for the stress field. That is,

$$\sigma(v) \approx \sigma(u) = K_I \sigma(u^I) + K_{II} \sigma(u^{II}) \tag{9}$$

Inserting Eqs. (7) and (9) to Eq. (6), and representing this formula separately with respect to MODE I and MODE II, following result can be obtained.

$$J = -\frac{1}{2} K_I \Phi(v, u^I, \phi) - \frac{1}{2} K_{II} \Phi(v, u^{II}, \phi) \tag{10}$$

where content of function $\Phi$ is

$$\Phi(v, u^\alpha, \phi) = \int_\Omega [\{\sigma_{i2}(u^\alpha)v_{i,2} - \sigma_{i1}(v)u^\alpha_{i,1}\} \phi_{,1}$$

$$- \{\sigma_{2i}(u^\alpha)v_{i,1} + \sigma_{i2}(v)u^\alpha_{i,1}\} \phi_{,2}] d\Omega \tag{11}$$

where, $\alpha = I, II$

After denoting $\sigma_{ij}(u^\alpha) = \sigma_{i,j}$ inserting Eqs. (7) and (9) to Eq. (11), following expressions for $\alpha = I, II$ can be obtained.

$$\Phi^I = \Phi(v, u^I, \phi) = K_I \Phi^I_1 + K_{II} \Phi^I_2$$

$$\Phi^{II} = \Phi(v, u^{II}, \phi) = K_I \Phi^{II}_1 + K_{II} \Phi^{II}_2 \tag{12}$$

$$\Phi^I_1 = \int_{\Omega^*} \{(\sigma^I_{i2} u^I_{i,2} - \sigma^I_{i1} U^I_{i,1}) \phi_{,1} - 2(\sigma^I_{2i} u^I_{i,1}) \phi_{,2}\} d\Omega$$

$$\Phi^I_2 = \int_{\Omega^*} \{(\sigma^I_{i2} u^{II}_{i,2} - \sigma^I_{i1} u^{II}_{i,1}) \phi_{,1} - (\sigma^I_{2i} u^{II}_{i,1} + \sigma^{II}_{2i} u^I_{i,1}) \phi_{,2}\} d\Omega$$

$$\Phi^{II}_1 = \int_{\Omega^*} \{(\sigma^{II}_{i2} u^I_{i,2} - \sigma^I_{i,1} u^{II}_{i,1}) \phi_{,1} - (\sigma^{II}_{2i} u^I_{i,1} + \sigma^I_{2i} u^{II}_{i,1}) \phi_{,2}\} d\Omega$$

$$\Phi_2^{II} = \int_{\Omega^*} \{(\sigma_{i2}^{II} u_{i,2}^{II} - \sigma_{i1}^{II} u_{i,1}^{II})\phi_{,1} - 2(\sigma_{2i}^{II} u_{i,1}^{II})\phi_{,2}\} \, d\Omega \tag{13}$$

By the way, $J$-integral value has the following relation with $K_I$ and $K_{II}$ in mixed mode.

$$J = \frac{(K_I)^2}{E^*} + \frac{(K_{II})^2}{E^*} \tag{14}$$

In this formula, $E^*$ is $E$ in plane stress condition and $E/(1-v^2)$ in plane strain condition respectively. In here, let $\Phi^I$ and $\Phi^{II}$ of Eq. (12) have components of MODE I, MODE II respectively, and equivalencing Eqs. (10) and (14), following expressions are obtained.

$$\Phi_1^I = -\frac{2}{E^*}, \quad \Phi_2^I = 0, \quad \Phi_1^{II} = 0, \quad \Phi_2^{II} = -\frac{2}{E^*} \tag{15}$$

So, the final expression obtaining $K_\alpha$ can be made from Eq. (12) as below.

$$K_\alpha = -\frac{E^*}{2}\Phi^\alpha = -\frac{E^*}{2}\Phi(\underset{\sim}{v}, \underset{\sim}{u}^\alpha, \phi), \quad \alpha = I, II \tag{16}$$

For the purpose of comparison with Babuška and Miller's proposal for $K_\alpha$, each term in Eq. (16) were replaced under hypothesis of plane strain condition. That result is as follows.

$$K_\alpha = -\frac{\mu}{1-v} \int_{\Omega^*} [\{\sigma_{i2}(\underset{\sim}{u}^\alpha) \, v_{i,2} - \sigma_{i1}(\underset{\sim}{v}) \, u_{i,1}^\alpha\}\phi_{,1}$$

$$-\{\sigma_{i2}(\underset{\sim}{u}^\alpha)v_{i,1} + \sigma_{i2}(\underset{\sim}{v})u_{i,2}^\alpha\}\phi_{,2}] \, d\Omega \tag{17}$$

### 2.2. Smooth curve function

In this study, a new smooth curve function of parabolic type was presented and comparison of results that are obtained from use of this function, Babuska and Miller's function, and Droz's function was given in various manners.

The smooth curve functions used are as follow.

(1) Function introduced here

$$\phi(r) = \begin{cases} 1 & ; \quad r \leq R_i \\ \dfrac{-1}{(R_e - R_i)^2}r^2 + \dfrac{2R_i}{(R_e - R_i)^2}r + \dfrac{R_e(R_e - 2R_i)}{(R_e - R_i)^2} & ; \quad R_i < r \leq R_e \end{cases} \tag{18}$$

(2) Babuška and Miller's function

$$\phi(r) = \begin{cases} 1 & ; \quad 0 \leq r < \frac{1}{2}R_e \\ 1 - 4\left(r - \dfrac{R_e}{2}\right)^2 / R_e^2 & ; \quad \frac{1}{2}R_e \leq r \leq R_e \end{cases} \tag{19}$$

(3) Droz's function

$$\phi(r) = \begin{cases} 1 - r^2/R_e^2 & ; \quad r < R_e \\ 0 & ; \quad r \geq R_e \end{cases} \tag{20}$$

In above, $R_i$ and $R_e$ denote the inner and outer integral radius respectively.

## 2.3. Surface integral method considering body forces

When body forces $f_i$ are considered in Fig. 1, *J*-integral over the domain $\Omega$ encompassed by the path is called *J'*-integral, and following expression can be made.

$$J' = \int_\Gamma (wn_1 - t_i u_{i,1}) ds - \int_\Omega f_i u_{i,1} d\Omega \tag{21}$$

And expression for the *J'*-integral over the $\Gamma_\varepsilon$ and $\Omega_\varepsilon$ is as follows.

$$J' = -\int_{\Gamma_\varepsilon} (wn_1 - t_i u_{i,1}) ds + \int_{\Omega_\varepsilon} f_i u_{i,1} d\Omega \tag{22}$$

In here, using smooth curve function, integral over the closed surface $\Omega^*$ can be expressed like below.

$$J' = -\int_{\Omega^*} f_i u_{i,1} \phi d\Omega - \int_{\Omega^*} \{(w - \sigma_{i1} u_{i,l}) \phi_{,1} - (\sigma_{i2} u_{i,1}) \phi_{,2}\} d\Omega + \int_{\Omega_\varepsilon} f_i u_{i,1} \phi d\Omega \tag{23}$$

By the way, since displacement $\underset{\sim}{v}$ obtained from the FEM analysis can be considered approximation of analytical solutions $\underset{\sim}{u}$, which are obtained from application of external forces and body forces together, following expression can be made.

$$\underset{\sim}{v} \approx \underset{\sim}{u} = \underset{\sim}{u}_g + k_I u' + k_{II} u''$$
$$\underset{\sim}{\sigma}(\underset{\sim}{v}) \approx \underset{\sim}{\sigma}(\underset{\sim}{u}) = \underset{\sim}{\sigma}_g + k_I \underset{\sim}{\sigma}' + k_{II} \underset{\sim}{\sigma}'' \tag{24}$$

In here, $\underset{\sim}{u}_g$, $\underset{\sim}{\sigma}_g$ mean displacement and stress by the application of the body forces only. Substituting Eq. (25) to Eq. (24) and then arranging, following expression can be obtained.

$$J' = K_I \left\{ -\frac{1}{2} \Phi(\underset{\sim}{v}, \underset{\sim}{u}', \phi) - \frac{1}{2} \psi(\underline{f}, \underset{\sim}{u}', \phi) \right\}$$

$$+ K_{II} \left\{ -\frac{1}{2} \Phi(\underset{\sim}{v}, \underset{\sim}{u}'', \phi) - \frac{1}{2} \psi(\underline{f}, \underset{\sim}{u}'', \phi) \right\} \tag{25}$$

here function $\psi$ is as follows.

$$\psi(\underline{f}, \underset{\sim}{u}^\alpha, \phi) = \int_{\Omega^*} f_i u_{i,1}^\alpha \phi d\Omega: \quad \alpha = I, \ II \tag{26}$$

In Eq. (26), since terms about MODE I and MODE II were separately represented, SIF, when considering body forces, could be obtained from the comparison Eq. (26) with Eq. (14). That is, following expression for $K^\alpha(\alpha = I, \ II)$ can be obtained.
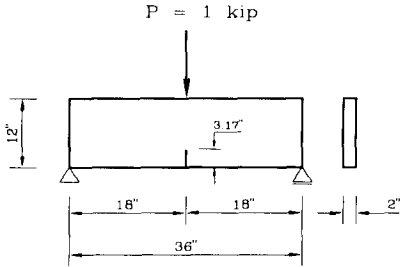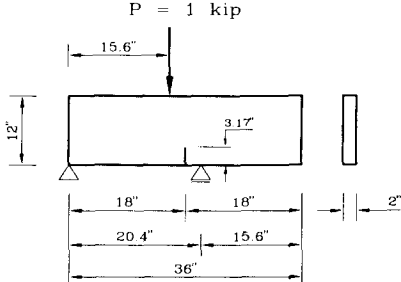
$$K_\alpha = -\frac{E^*}{2} \Phi(\underset{\sim}{v}, \underset{\sim}{u}^\alpha, \phi) - \frac{E^*}{2} \psi(\underline{f}, \underset{\sim}{u}^\alpha, \phi), \quad \alpha = I, \ II \tag{27}$$

# 3. Numerical example and consideration

## 3.1. Programming

In here, contents of computer program pertaining to differentiation and numerical integration

Table 1 Numerical example: simple beam with concentrated load



| Model | No. of elements | No. of points | Aspect ratio |
|---|---|---|---|
| A | 48 | 179 | 1.00 |
| B | 84 | 297 | 0.50 |
| C | 338 | 1101 | 0.24 |

| Model | No. of elements | No. of points | Aspect ratio |
|---|---|---|---|
| D | 48 | 179 | 1.00 |
| E | 84 | 297 | 0.50 |
| F | 338 | 1101 | 0.24 |
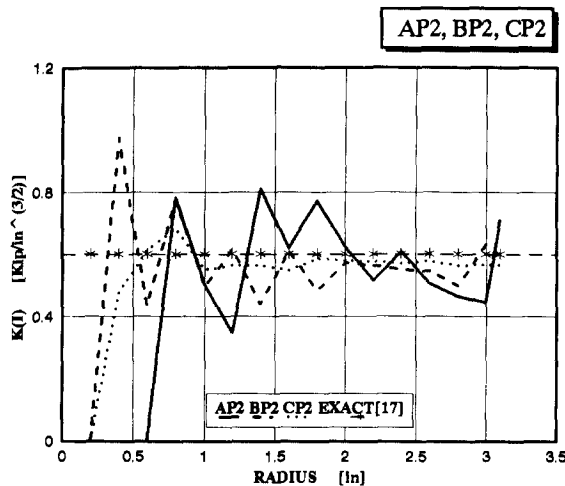


Fig. 2 AP2, BP2, CP2
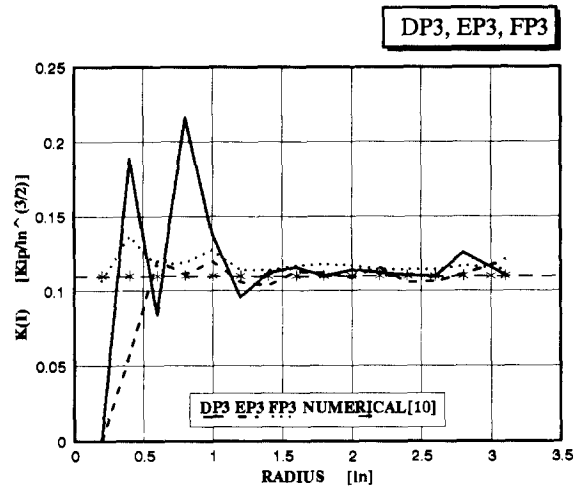


Fig. 3 DP3, EP3, FP3

with respect to various functions in Eq. (16) and Eq. (27) were not represented in order to be brief. It can be seen that SIF is calculated by using FEM results as a input data in this program.

## 3.2. Simple beam with concentrated load

In this paper, results obtained only from simple beam with concentrated load (Table 1) in pure mode and mixed mode were represented due to limited pages. Size of the beam used in the numerical example is 36 in. length and 2 in. thickness, and the beam has central crack of 3.17 in. depth in lower edge. And aspect ratio appeared in Table 1 means ratio of element length at the crack tip with reference to crack length.

Various results obtained from the numerical analysis were given in below. To begin with, explanation about titles used in Fig.2 to Fig.22 is necessary. That is, first character means model
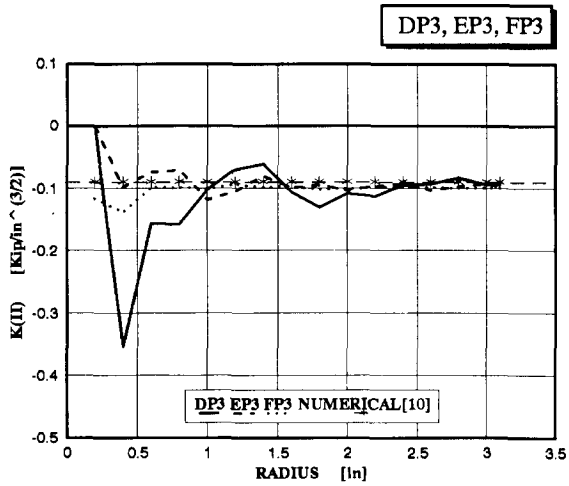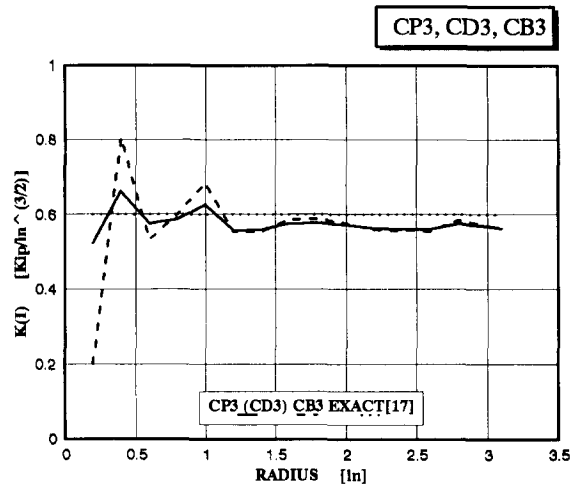
Fig. 4 DP3, EP3, FP3
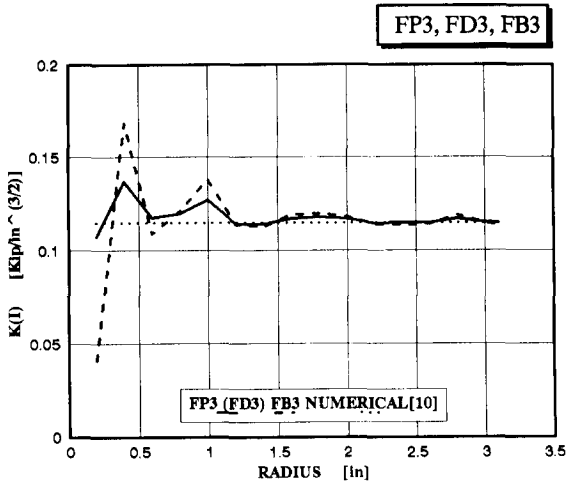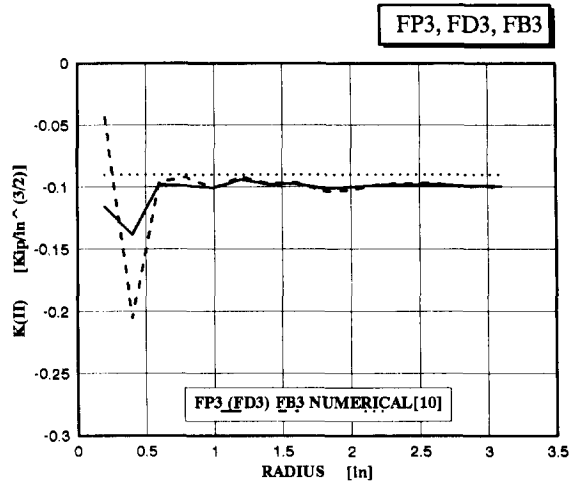


Fig. 5 CP3, CD3, CB3



Fig. 6 FP3, FD3, FB3



Fig. 7 FP3, FD3, FB3

name, and the second represents kinds of smooth curve function used in this program, in which P, B, and D mean this study's function, Babuška and Miller's function, and Droz's function respectively. And number 2, 3, etc. appeared in third place means number of gauss points used in numerical integration. Finally, fourth character is used only in case of necessity. That is, B means consideration of body forces and I means investigation according to variance of inner integral radius.

For MODE I case, degrees of convergence with respect to magnitude of mesh sizes were compared in Fig.2. In the figure, the axis of abscissa and ordinate represent outer integral radius and SIF respectively. A 2×2 integration and this study's smooth function were used in above calculation. For this problem, analytical solution $K_I=0.6011$ kip/in$^{3/2}$ (Ewalds and Wanhill 1984) was investigated. For mixed mode, calculation results obtained by 3×3 integration were given at Fig. 3 and Fig. 4. Numerical results for this problem were $K_I=0.1132$ kip/in$^{3/2}$, $K_{II}=-0.089$
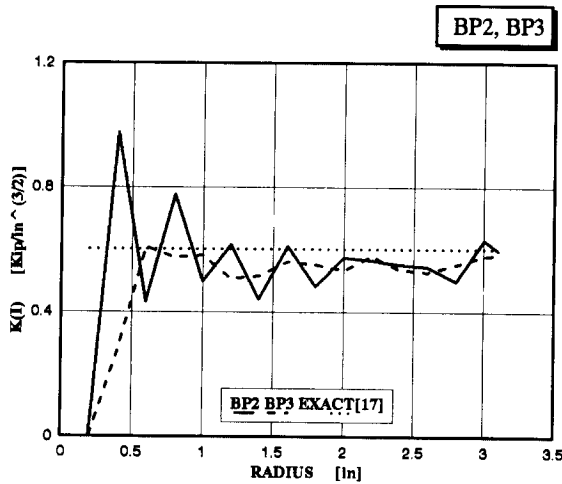
BP2, BP3

BP2 BP3 EXACT[17]
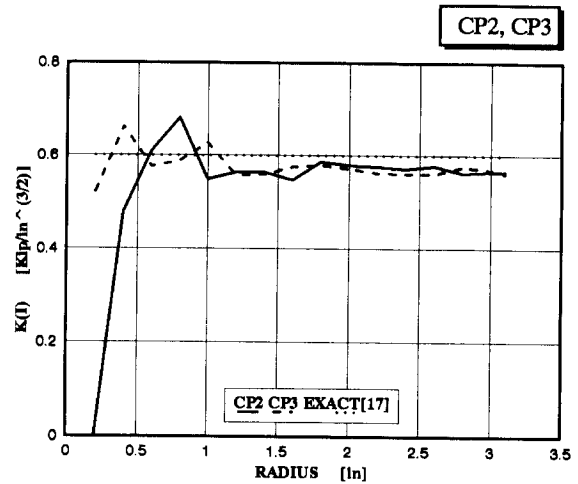
Fig. 8 BP2, BP3

CP2, CP3

CP2 CP3 EXACT[17]

Fig. 9 CP2, CP3

EP2, EP3

EP2 EP3 NUMERICAL[10]

Fig. 10 EP2, EP3

EP2, EP3

EP2 EP3 NUMERICAL[10]
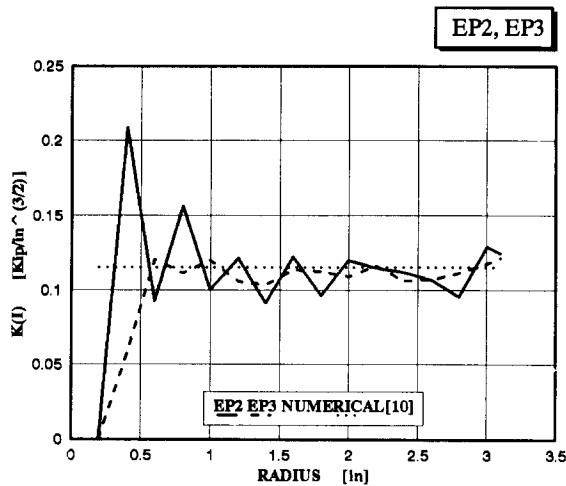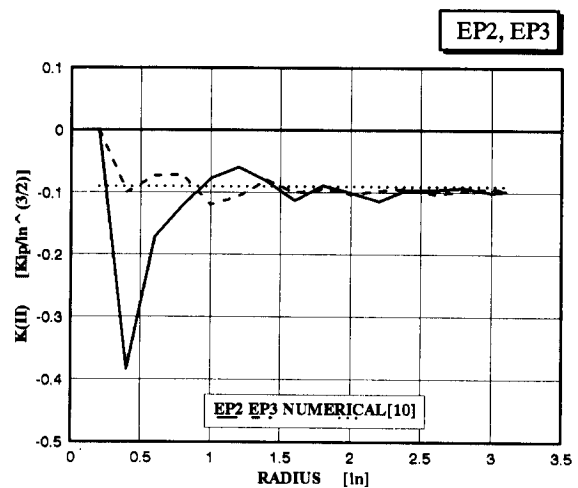
Fig. 11 EP2, EP3

kip/in$^{3/2}$ (Jin, Jang, Choi and Eum 1989). From these figures, it could be known that the more fine mesh were used, the more rapid convergence were obtained.

Effectiveness of this study's smooth curve function was tested to model C and model F by 3×3 integration, and these calculation results were given in Fig. 5 through Fig. 7. To be seen in these figures, results were similar to ones obtained from the use of Babuška and Miller's function. In here, results by Droz's function were not plotted in another way, since Droz's function is equal to one obtained by setting $R_i = 0$ for this study's function.

In Fig. 8 through Fig. 13, results obtained from being outer integral radius varied and inner integral radius fixed to zero likewise in the case of Fig. 2 through Fig. 7 were plotted. For $K_I$ and $K_{II}$, degrees of convergence were excellent in the region 1/3 $Re_{max} \sim Re_{max}$, where $Re_{max}$ means crack length. From these figures, it could be known that more excellent results were obtained by the use of fine mesh generation and 3×3 integration.

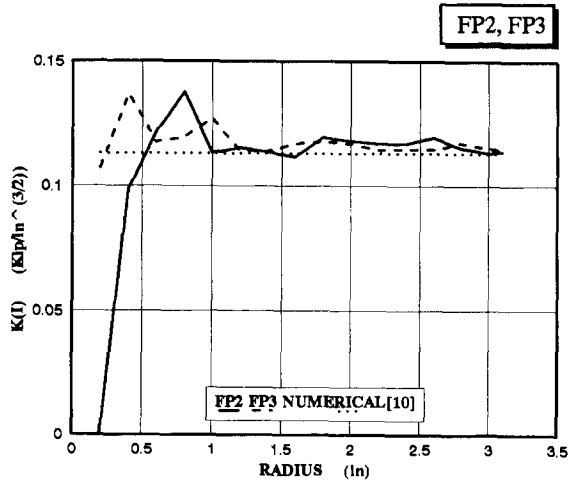In Fig. 14 through Fig. 16 results obtained by fixing external radius to crack length and by
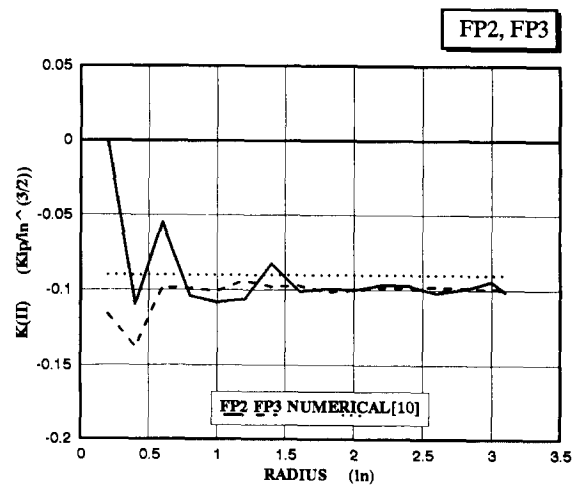
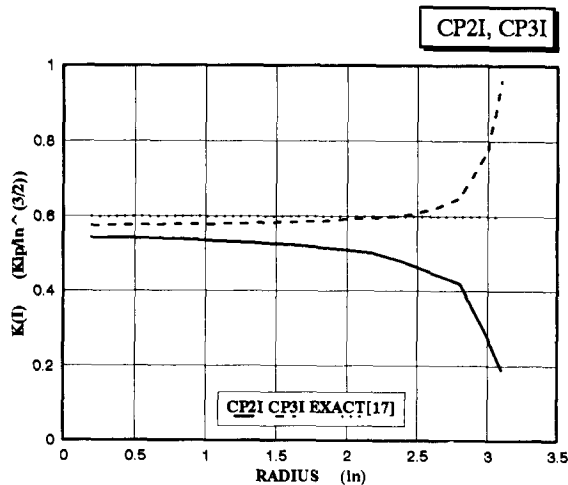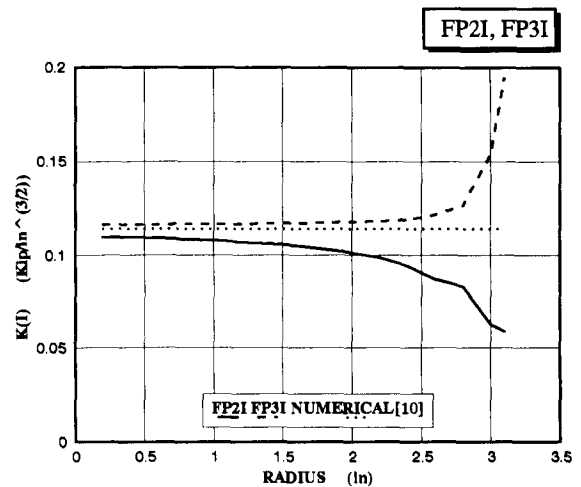Fig. 12 FP2, FP3



Fig. 13 FP2, FP3



Fig. 14 CP2I, CP3I



Fig. 15 FP2I. FP3I

incrementing inner radius gradually from zero to crack length were given. In here, it could be known that very similar values to exact ones were obtained right away but the values were diverged when inner radius were more than about 2/3 $Re_{max}$. The reason for above results may be thought as a reduction of the integral area. That is, it can be thought that number of integral points are not sufficient to express properties of surface integral.

Also, cases considering body forces ($0.839 \times 10^{-4}$ kip/in$^3$) were studied. Numerical solutions obtained from other numerical technique for this problem were $K_I = 0.6181$ kip/in$^{3/2}$ in MODE I, and $K_I = 0.1006$ kip/in$^{3/2}$, $K_{II} = -0.0940$ kip/in$^{3/2}$ mixed mode. Calculation results were plotted in Fig. 17 through Fig. 19, and it could be seen from these figures that degrees of convergence were excellent.

In Fig. 20 through Fig. 22 results obtained by $2 \times 2$, $3 \times 3$, $4 \times 4$, $5 \times 5$ numerical integrals for the same model were given. In here, it could be known that results obtained by $4 \times 4$ and $5 \times 5$ integrals had not any other good performance with respect to the results obtained by $3 \times 3$ integral.
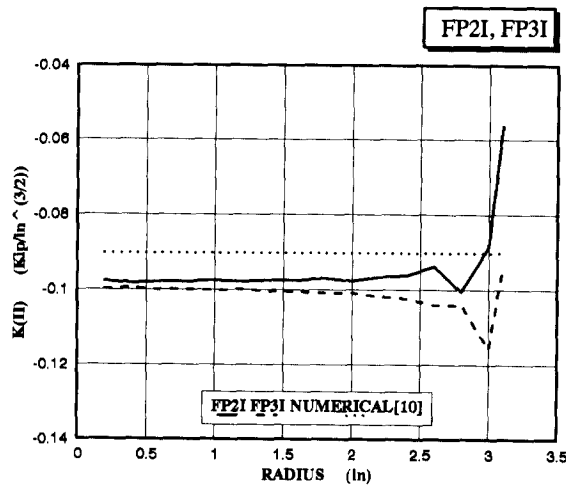
FP2I, FP3I



Fig. 16 FP2I, FP3I

CP2B, CP3B



Fig. 17 CP2B, CP3B

FP2B, FP3B
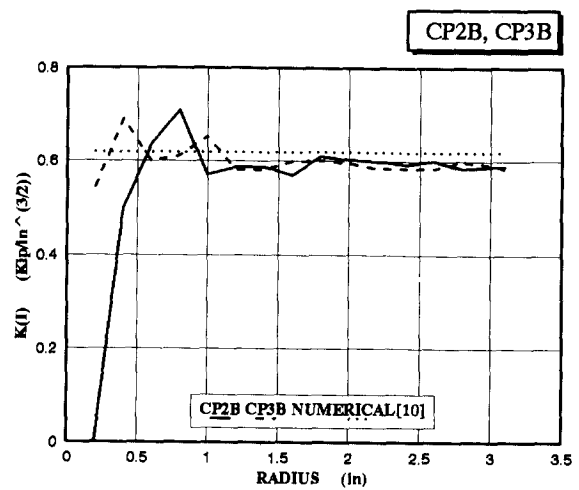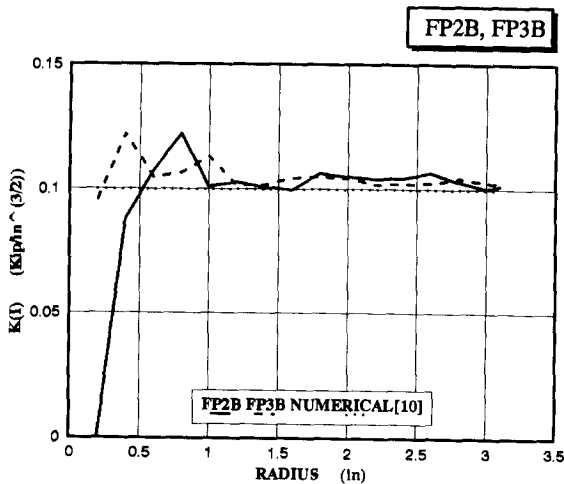

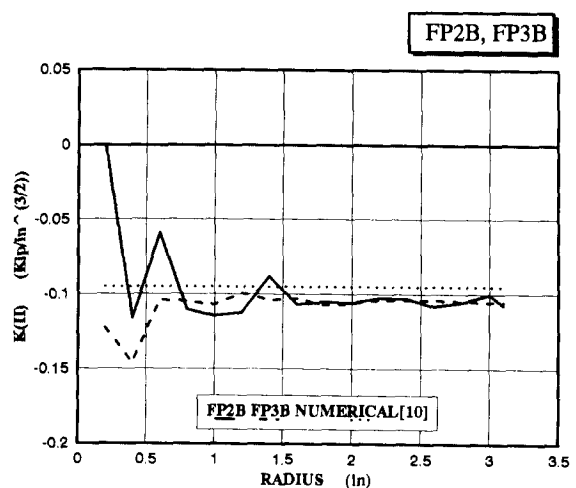
Fig. 18 FP2B, FP3B

FP2B, FP3B



Fig. 19 FP2B, FP3B

A tensioned-plates which have a notch in one edge were analyzed for the purpose of comparison with the Droz's results. From the comparison, it could be known that Droz's results had quite a few differences with respect to analytical solution or numerical solution, and then this study's results are more excellent.

## 4. Conclusions

In this study, to determine the stress intensity factors used in LEFM more easily, a general formulation based on the surface integral method was induced and then a computer program related was studied. In this program, surface integral was being carried out by preparing results of FEM analysis, using not singular elements but general 8-noded isoparametric elements at the crack tip, as a input data.
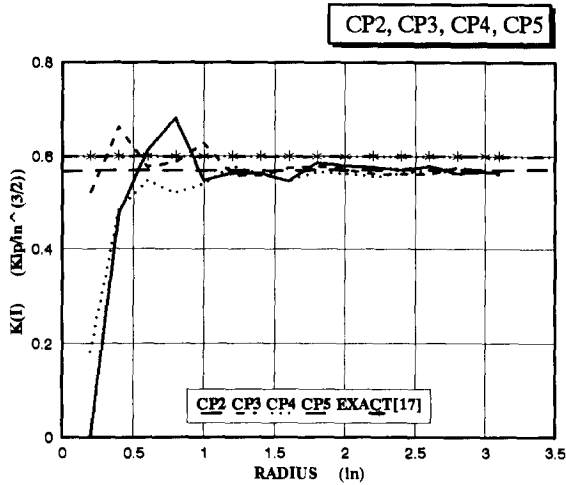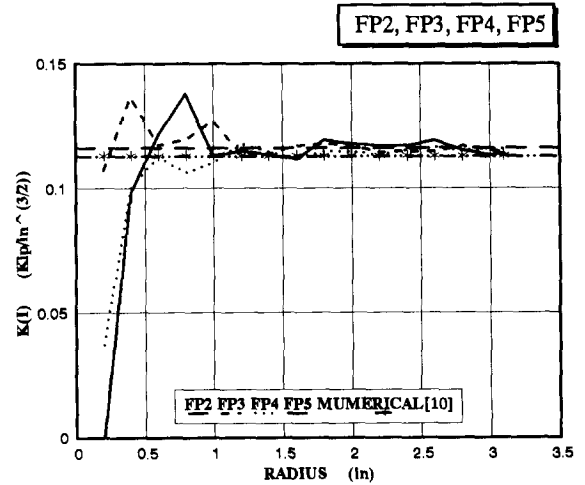
Fig. 20 CP2, CP3, CP4, CP5
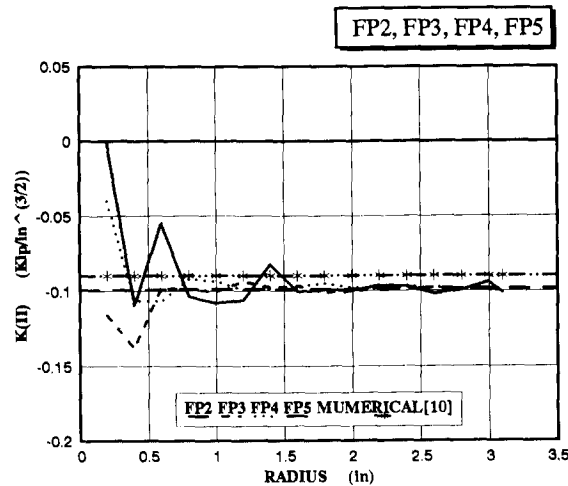


Fig. 21 FP2, FP3, FP4, FP5



Fig. 22 FP2, FP3, FP4, FP5

(1) A new smooth curve function was suggested and above surface integral method was extended to the case where body forces act.

(2) By the use of smooth curve function proposed in this study and conventional element meshes in which the aspect ratio (element length at the crack tip/crack length) is about 25%, very similar $K_I$ and $K_{II}$ values to the theoretical one or other numerical ones could be obtained for the outer radius ranging from $1/3 \; Re_{max}$ to $Re_{max}$ and for the inner radius zero.

(3) In the variation of the inner integral radius from zero to $Re_{max}$, fixing the outer radius to $Re_{max}$, results approximating to the exact values were obtained directly. But it could be seen that the results are diverged when the inner radius are larger than about $2/3 \; Re_{max}$ due to reduction of the integral area.

(4) In the numerical integration, more excellent results could be obtained in $3 \times 3$ integral

than in 2×2 integral, but there are little differences between 3×3 integral and over 4×4 integrals.

## References

Atluri, S.N. (1982), "Path independent integrals in finite elasticity and inelasticity, with body forces, inertia and arbitrary crack force conditions", *Eng. Fract. Mech.,* **16**(3), 341-364.

Babuška, I. and Miller, A. (1984), "The post-processing approach in the finite element method - Part 1: Calculation of displacements, stresses and other higher derivatives of the displacements", *International Journal for Numerical Methods in Engineering,* **20**, 1085-1109.

Babuška, I. and Miller, A. (1984), "The post-processing approach in the finite element method - Part 2: The calculation of stress intensity factors", *International Journal for Numerical Methods in Engineering,* **20**, 1111-1129.

Barsoum, R.S. (1976), "On the use of isoparametric finite elements in linear fracture mechanics", *International Journal for Numerical Methods in Engineering,* **10**, 25-37.

Carpinteri, A. (1985), "Scale effects in fracture of plain and reinforced concrete structures", *Fracture Mechanics of Concrete* (Sih,G.C. and DiTommaso,A.Ed.), Martinus Nijhoff Publishers, 95-140.

Droz, P. (1987), "Modele numerique du comportement non-lineaire d'ouvrages massifs en beton non arme", *pour l'obtention du grade de docteur es sciences techniques,* Ecole Polytechnique Federale de Lausanne, 1-148.

Ewalds, H.L. and Wanhill, R.J.H. (1984), *Fracture mechanics,* Edward Arnold Ltd., 97.

Hellen, T.K. (1975), "On the method of virtual crack extensions", *International Journal for Numerical Methods in Engineering,* **9**, 187-207.

Hillerborg, A. (1985), "Numerical methods to simulate softening and fracture of concrete", *Fracture Mechanics of Concrete* (Sih, G.C. and DiTommaso, A. Ed.), Martinus Nijhoff Publishers, 141-170.

Ingraffea, A.R. and Saouma, V.E. (1985), "Numerical modeling of discrete crack propagation in reinforced and plain concrete", *Fracture Mechanics of Concrete* (Sih, G.C. and DiTommaso,A. Ed.), Martinus Nijhoff Publishers, 171-225.

Irwin, G.R. (1956), "Onset of fast crack propagation in high strength steel and aluminum alloys", *Sagamore Research Conference Proceedings,* **2**, 289-305.

Jin, C.S., Jang, H.S., Choi, H.T. and Eum, J.S. (1989), "Mixed mode crack propagation models of the concrete structures(I)", *Research Paper of College of Engng.,* Pusan Nat'l Univ., **38**, 83-91.

Kaplan, M.F. (1961), "Crack propagation and the fracture of concrete", *Journal of the American Concrete Institute,* **58**, 591-610.

Kesler, C.E., Naus, D.J. and Lott, J.L. (1972), "Fracture mechanics - Its applicability to concrete, in mechanical behaviour of materials", *The Society of Materials Science,* **IV**, Japan, 113-124.

Kishimoto, K., Aoki, S. and Sakata, M. (1980), "On the path independent integral-J^", *Engineering Fracture Mechanics,* **13**, 841-850.

Mindess, S. (1983) "The cracking and fracture of concrete: an annotated bibliography 1928-1981", *Fracture Mechanics of Concrete* (Wittmann F.H. Ed.) Elsevier, 539-661.

Neville, A.M. (1959), "Some aspects of the strength of concrete", *Civil Engineering,* part I; **54**, 1153-1156.

Owen, D.R.J. and Fawkes, A.J (1983), "Engineering fracture mechanics", Pineridge Press Ltd., 1-305.

Parks, D.M. (1974), "A stiffness derivative finite element technique for determination of crack tip stress intensity factors", *International Journal of Fracture,* **10**(4), 487-502.

Rice, J.R. (1968), "A path independent integral and the approximate analysis of strain concentration by notches and cracks", Transactions of the ASME, *Journal of Applied Mechanics,* 379-386.

Saouma, V.E., Ingraffea, A.R. and Catalano, D.M. (1982), "Fracture toughness of concrete: revisited", *Journal of the Engineering Mechanics Division, ASCE,* **108**, 1152-1166.

Sih, G.C. (1984), "Mechanics of material damage in concrete", *Fracture Mechanics of Concrete* (A. Carpinteri and A.R. Ingreffea, Ed.), Martinus Nijhoff Publishers, 1-28.